



# Techno-economic feasibility assessment of calcium looping combustion using commercial technology appraisal tools

Sebastian Michalski\*, Dawid P. Hanak, Vasilije Manovic

Energy and Power, School of Water, Energy and Environment, Cranfield University, Cranfield, Bedfordshire, MK43 0AL, UK

## ARTICLE INFO

### Article history:

Received 22 November 2018

Received in revised form

30 January 2019

Accepted 5 February 2019

Available online 11 February 2019

### Keywords:

Efficiency penalty

Carbon capture

Clean power technologies

Clean coal

Economic assessment framework

Carbonate looping

## ABSTRACT

Calcium looping combustion (CaLC) is a new class of low- $\text{CO}_2$ -emission technologies for thermo-chemical conversion of carbonaceous fuels that can help achieve the emissions reduction targets set out in the Paris Agreement. Compared to mature  $\text{CO}_2$  capture technologies, which cause net efficiency penalties higher than 7% points, CaLC results in a net efficiency penalty of 2.9% points. However, a thorough economic assessment of CaLC needs to be undertaken to evaluate its economic viability. The levelised cost of electricity is commonly used to assess the economic performance of clean energy systems. However, this method does not account for commercially important parameters, such as tax, interest, and depreciation charges. This study aimed to improve the reliability and accuracy of economic assessments of clean energy systems by implementing the net present value (NPV) approach. This approach was applied to assess the economic performance of two concepts of the CaLC-based power plant with either the conventional steam cycle (SC) or the supercritical  $\text{CO}_2$  cycle (s- $\text{CO}_2$ ) for heat utilisation along with the bottom-up approach to total capital cost estimation. A parametric study for both concepts was also conducted to assess the impact of the key thermodynamic parameters on the economic performance. Although the s- $\text{CO}_2$  case with revised assumptions was shown to result in a 1%-point lower net efficiency compared to the SC case, its break-even cost of electricity was lower by 0.81 €/MWh. Further improvements of the techno-economic performance can be sought by optimisation of the s- $\text{CO}_2$  cycle structure.

© 2019 The Authors. Published by Elsevier Ltd. This is an open access article under the CC BY license (<http://creativecommons.org/licenses/by/4.0/>).

## 1. Introduction

To reduce the risks and impacts of climate change, which is one of the most important challenges globally, the temperature increase needs to be kept well below 2 °C (2DS) compared to pre-industrial levels (Tollefson, 2015). The power sector accounts for a third of total greenhouse gas emissions (International Energy Agency, 2016), primarily since 28.1% of global electricity is produced from coal (International Energy Agency, 2017a). To meet the long-term 2DS objectives by 2050, 14% of total  $\text{CO}_2$  emissions reduction needs to be achieved by implementation of carbon capture and storage (CCS) technologies (International Energy Agency, 2017b). In addition, the total emission reduction cost is predicted to be 70% (Department of Energy and Climate Change, 2012), or even 140% (Global CCS Institute, 2017) higher in scenarios without CCS. However, it should be noted that a larger part of the emission

reduction is related to an increase in the process efficiency (40%) and use of renewable energy sources (35%) (International Energy Agency, 2017b).

In recent years, significant progress has been achieved in reducing the energy intensity of CCS. Unfortunately, the mature  $\text{CO}_2$  capture and separation technologies are still expected to cause a net efficiency penalty of at least 7% points compared to conventional power plants without  $\text{CO}_2$  capture (Boot-Handford et al., 2014; Hanak et al., 2015a, 2015c). Such efficiency penalty and high investment costs would lead to an increase in the cost of electricity of at least 60% (Renner, 2014). It has also been estimated that, regardless that CCS processes are designed to remove 90% of  $\text{CO}_2$  from the flue gas (Singh et al., 2011), the implementation of mature CCS technologies on fossil-fuel-fired power plants will reduce their  $\text{CO}_2$  emissions by only 60–80% over the process lifetime (Koornneef et al., 2008; Singh et al., 2011). This is caused by the drop in the net efficiency due to implementation of CCS. Therefore, to achieve the same power output, the size of the fossil-fuel-fired power plant and its fuel consumption need to be

\* Corresponding author.

E-mail address: [s.s.michalski@cranfield.ac.uk](mailto:s.s.michalski@cranfield.ac.uk) (S. Michalski).

increased, thus causing higher CO<sub>2</sub> emissions. The net efficiency penalty can be reduced by development of emerging technologies, such as calcium looping (CaL) (4–8% points) (Hanak et al., 2015a; Perejón et al., 2016; Romeo et al., 2008), currently tested at pilot-plant scale (Arias et al., 2013; Chang et al., 2014; Sánchez-Biezma et al., 2013; Ströhle et al., 2014). Yet, the key limitation of this technology is associated with degradation of the sorbent performance with a number of calcination and carbonation cycles. This is primarily due to sintering, attrition and sulphation of the sorbent that impose the requirement for sorbent make-up to maintain desired average sorbent conversion in the carbonator (Dean et al., 2011). Similarly, lower efficiency penalties can also be achieved by novel concepts such as the oxy-combustion power plant using an air separation unit (ASU) based on ion transport membranes (Kotowicz and Michalski, 2016, 2015). Further reduction of the net efficiency penalty (to 2.9% points) can be achieved by development of standalone calcium looping combustion (CaLC) technology based on indirect heat transfer from the air-fired combustor to the calciner (Hanak and Manovic, 2017a).

The high emission intensity of the current power plant fleet results not only from outdated combustion systems, but primarily from wide use of relatively inefficient conventional steam cycles for conversion of thermal energy into electricity. The net efficiency can be further increased by approximately 0.1% point on modification of the heat recovery systems (Kotowicz and Michalski, 2016) and development of more efficient steam turbines, or by several percentage points through increased live steam parameters (Kotowicz and Michalski, 2016). Unfortunately, these changes significantly increase the investment costs and are limited by currently available materials. Replacing the conventional steam cycles with advanced power cycles, following the recent developments in solar and nuclear power plants, can be a less expensive approach to increase the net efficiency of fossil-fuel-fired power plants (Marchionni et al., 2017). This is because application of the closed Brayton cycles based on different working media (CO<sub>2</sub>, He or Xe) can achieve similar (or even higher) efficiencies to the steam cycles with lower investment costs and higher power-to-cubature ratio, also known as a power density [MW/m<sup>3</sup>].

The economic assessment is even more important than thermodynamic assessment to evaluate the commercial attractiveness of considered technology. Yet, the data supporting the economic feasibility of the CaL concepts appear to be limited in the open literature, especially for the novel concepts such as CaLC (Hanak et al., 2018b). Moreover, the economics of the CaL concepts is usually evaluated using the levelised cost of electricity (LCOE) method, presented in Eq. (1). The LCOE depends on two thermodynamic parameters (Abanades et al., 2007; Cormos, 2014; Hanak and Manovic, 2017a): the net power output of the power plant ( $P_N$ ) and net efficiency of the power plant ( $\eta_N$ ). It also depends on the capacity factor (CF), the specific fuel cost (SFC) and the specific variable operating and maintenance cost (VOM). Finally, to calculate the LCOE, the total capital requirement (TCR), fixed operating and maintenance cost (FOM) and fixed charge factor (FCF) need to be estimated. Therefore, this method is simple to implement and is widely used to evaluate the economic performance of clean energy systems.

$$LCOE = \frac{TCR \cdot FCF + FOM}{P_N \cdot CF \cdot 8760} + VOM + \frac{SFC}{\eta_N} \quad (1)$$

The recent studies of the CaL concepts (Hanak et al., 2018b; Hanak and Manovic, 2017b) have indicated that CaL retrofits to fossil-fuel-fired power generation systems have been most often reported to result in LCOEs between 50 and 75 €/MW<sub>el</sub>h, with the corresponding cost of CO<sub>2</sub> avoided (AC) being reported to be

between 10 and 30 €/tCO<sub>2</sub> (Hanak et al., 2018b). The LCOEs reported in the literature (Abanades et al., 2007; Cormos and Cormos, 2017; Cormos, 2014; Hanak et al., 2016; Mantripragada and Rubin, 2013; Romano et al., 2013; Romeo et al., 2008; Yang et al., 2010) are summarised in Fig. 1. The significant difference in reported values is mainly caused by discrepancies in the specific total capital requirement and net efficiency of the base power plant (different live and reheated steam parameters) (Hanak and Manovic, 2017b). The highest capital requirement (3723 €/kW<sub>el, gross</sub>) is considered by Mantripragada and Rubin (2013) while the lowest value (1305 €/kW<sub>el, gross</sub>) is reported by Abanades et al. (2007).

Therefore, the economic performance of the CaL retrofits is typically reported to be superior to chemical solvent scrubbing (LCOE = 65–89 €/MW<sub>el</sub>h; AC = 35–75 €/tCO<sub>2</sub>) (Cormos and Cormos, 2017; Mac Dowell and Shah, 2015; Rubin et al., 2015; Versteeg and Rubin, 2011; ZEP, 2011) and comparable to oxy-fuel combustion (LCOE = 55–75 €/MW<sub>el</sub>h; AC = 35–75 €/tCO<sub>2</sub>) (Cormos, 2016; Hanak et al., 2017) retrofits. Moreover, despite a limited amount of data in the current literature, the LCOE and the cost of CO<sub>2</sub> avoided associated with the CaL-based power generation systems, such as CaLC, are most likely to be within 50–100 €/MW<sub>el</sub>h and 10–50 €/tCO<sub>2</sub>, respectively (Hanak et al., 2018b). It needs to be highlighted, however, that the economic appraisal of commercial projects is commonly performed by employing the net present value (NPV) approach (Pike et al., 2015). As opposed to the LCOE, the NPV approach considers annual discounted cash flows, including tax, interest, and depreciation charges, and allows estimating a number of break-even points, such as break-even price of electricity or break-even carbon tax. An additional benefit of the NPV method is that it can form a basis for an advanced economic analysis, such as economic risk analysis (Kotowicz and Michalski, 2015).

This study aims to improve the reliability and flexibility of the economic assessment of the CaLC-based power plant concepts employing either the conventional steam cycle (SC) or advanced power cycles, such as the supercritical CO<sub>2</sub> cycle (s-CO<sub>2</sub>). This is achieved by adapting the NPV approach to assess the economic performance of the considered concepts, in contrast to the LCOE approach commonly used in the literature. Furthermore, a bottom-up cost estimation method for the total investment cost of the CaLC-based power plant has been derived, which takes into consideration the capital cost of each piece of equipment and allows evaluating systems with different types and structures of advanced power cycles. The equipment capital costs are estimated considering the thermodynamic parameters, which have the largest impact on the equipment size, as the scaling factors. Thus, a

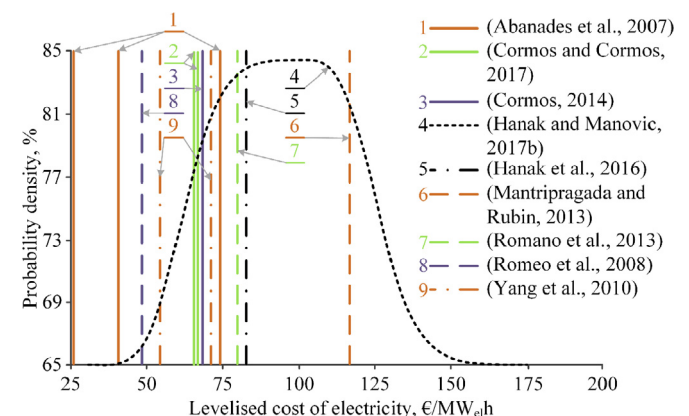


Fig. 1. LCOE values for power plants retrofitted with CaL. (Adapted with permission from Hanak and Manovic (2017b). Copyright, 2017 Elsevier).

change of thermodynamic parameters is reflected in the break-even electricity price. This is shown in the parametric analysis of the considered CaLC-based power plant concepts.

## 2. Process description

### 2.1. Calcium looping combustion with a supercritical steam cycle

The 594.2 MW<sub>el, gross</sub> low-CO<sub>2</sub>-emission power plant based on CaLC proposed by Hanak and Manovic (2017a), modelled in Aspen Plus® (AspenTech, 2017), is used as a reference case in this work (Fig. 2). The coal-fired combustor is assumed to operate at 1000 °C, to ensure efficient heat transfer to the calciner operating at 900 °C. The indirect heat transfer can be facilitated via either a heat transfer wall (Abanades et al., 2005) or heat pipes (Junk et al., 2016, 2013). The RMU ratio (Eq. (2)), which is a ratio of the molar flow rate of fresh limestone make-up ( $\dot{n}_{MU}$ ) and solid looping rate at the inlet to the carbonator ( $\dot{n}_{LR}$ ), was assumed to be 3%. The RMU is then used to calculate the maximum average conversion using the model derived by Rodríguez et al. (2010), which utilises the semi-empirical correlation proposed by Li et al. (2008). The sorbent deactivation curve is assumed based on the measurements from the 1.7 MW<sub>th</sub> la Pereda pilot plant (Sánchez-Biezma et al., 2013).

$$RMU = \frac{\dot{n}_{MU}}{\dot{n}_{LR}} \quad (2)$$

The only modification of the CaLC model developed earlier by Hanak and Manovic (2017a) is replacement of the equivalence ratio specification with the constant O<sub>2</sub> content specification in the dry flue gas (2%<sub>vol</sub>) to reflect the more realistic process control approach. The considered coal has a higher heating value (HHV) of 27.01 MJ/kg and the following composition: carbon – 64.54%; sulphur – 2.54%; hydrogen – 4.55%; nitrogen – 1.27%; oxygen – 6.97%; chlorine – 0.30%; ash – 9.82%; and moisture – 10.01%.

Flue gas from the combustor is then fed to the carbonator for CO<sub>2</sub> removal. It is assumed that this unit operates at a total CO<sub>2</sub> capture level of 90%, considering both CO<sub>2</sub> from fuel combustion and calcination of make-up sorbent. To achieve this, 88.6% of the CO<sub>2</sub> is captured in the carbonator. The operating temperature of the carbonator is assumed to be 650 °C. The concentrated CO<sub>2</sub> stream from the calciner is fed to the CO<sub>2</sub> compression unit that consists of a nine-stage intercooled compressor (with polytropic efficiency of 77–80% and intercooling to 40 °C with heat transfer coefficient of 300 W/m<sup>2</sup>°C), and a pump (with isentropic efficiency of 85%). The

mechanical efficiency of the pump and compressor is 99.6%. Pressure of 110 bar is assumed at the outlet of the CO<sub>2</sub> compression train (CCT). Other assumptions regarding the operating conditions of CaLC are gathered in Table 1.

In the reference case, the heat available in CaLC (flue gas stream, carbonator and clean gas stream) is used to raise high-pressure steam in the conventional steam cycle. The live and reheat steam parameters of such cycle are 593.3 °C/24.2 MPa and 593.3 °C/4.9 MPa, respectively. The final feed water temperature is 289.5 °C. Other assumptions concerning the conventional steam cycle, heat exchangers and CO<sub>2</sub> compressor unit are gathered in Table 1. Importantly, the cases considered in this work assume that there is no heat loss in the heat exchangers.

### 2.2. Calcium looping combustion system with s-CO<sub>2</sub> cycle

This work aims to use the NPV method to assess the feasibility of using the s-CO<sub>2</sub> cycle in place of the conventional SC to utilise the heat available from CaLC. The current literature reports that the s-CO<sub>2</sub> cycles are characterised by higher thermal cycle efficiencies than that of the conventional SCs (Hanak and Manovic, 2016; Wang and Dai, 2016). Additionally, parameters such as relatively higher density of s-CO<sub>2</sub> and lower pressure ratios lead to a significant reduction in the size of the cycle equipment, hence, lower capital costs compared to the conventional SCs (Marchionni et al., 2017; Zhang et al., 2018). Therefore, it is expected that integration of the s-CO<sub>2</sub> cycle to CaLC will further improve its economic performance. It is assumed that CaLC and CCT have the same structure as the reference case presented in Fig. 2 (Hanak and Manovic, 2017a), and are based on the same design specifications and assumptions as detailed in Section 2.1 and Table 1. The only difference is that the heat available in CaLC is used in the s-CO<sub>2</sub> cycle, as shown in Fig. 3.

The considered s-CO<sub>2</sub> cycle is a closed Brayton cycle using CO<sub>2</sub> in a supercritical state as a working medium. The thermodynamic model of the cycle was developed in Aspen Plus® (AspenTech, 2017). The s-CO<sub>2</sub> cycle model was developed by Hanak and Manovic (2016) and validated with the results presented by Le Moulec (2013) and experimental data provided by Park et al. (2018). Importantly, the latter confirmed that the s-CO<sub>2</sub> model used in this work accurately represents the experimental data and is in line with the validation results presented by Park et al. (2018). The s-CO<sub>2</sub> model was then modified for the purpose of this work, as detailed below.

In the considered s-CO<sub>2</sub> cycle, the main compressor, with an isentropic efficiency of 85%, increases the pressure of the CO<sub>2</sub> stream from 7.4 MPa to 20 MPa. Then, the main stream is divided into two separate streams feeding the low-temperature clean gas cooler (CGC) and low-temperature heat recuperator (LTR). The former heat exchanger reduces the clean gas temperature to arrive at a temperature difference at the cold end of the heat exchanger of 20 °C. The latter heat exchanger recovers the heat from the CO<sub>2</sub> stream leaving the high-temperature recuperator (HTR), before it enters the cooler. It is assumed that the cold-end temperature difference is 5 °C. The split ratio of the CO<sub>2</sub> stream is adjusted to arrive at the LTR hot-end temperature difference of 5 °C. The validity of this assumption was checked in the parametric study presented in Section 4.2. Both streams are then mixed and fed to the HTR, for which a cold-end temperature difference of 5 °C was assumed. The preheated supercritical CO<sub>2</sub> stream is then further heated in three carbonator heat exchangers: the first cooling down clean gas; the second located in the reaction zone; and the third cooling down the flue gas before it enters the carbonator. The cold-end temperature difference of 20 °C is assumed in the first clean gas cooler. As a result, the live supercritical CO<sub>2</sub> stream leaves the heat exchanger network at 600 °C. It is then fed into an expander with

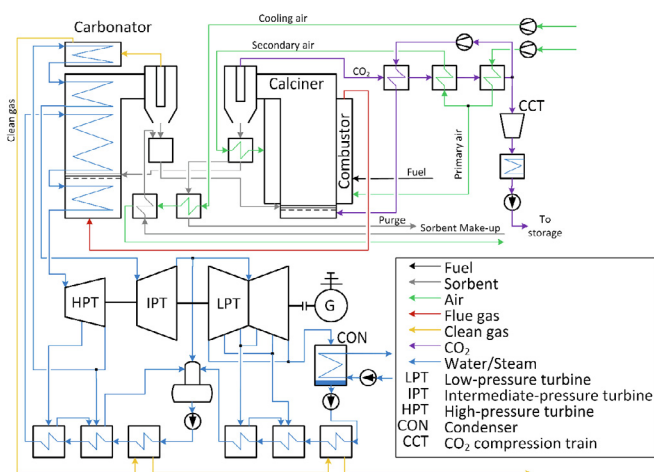
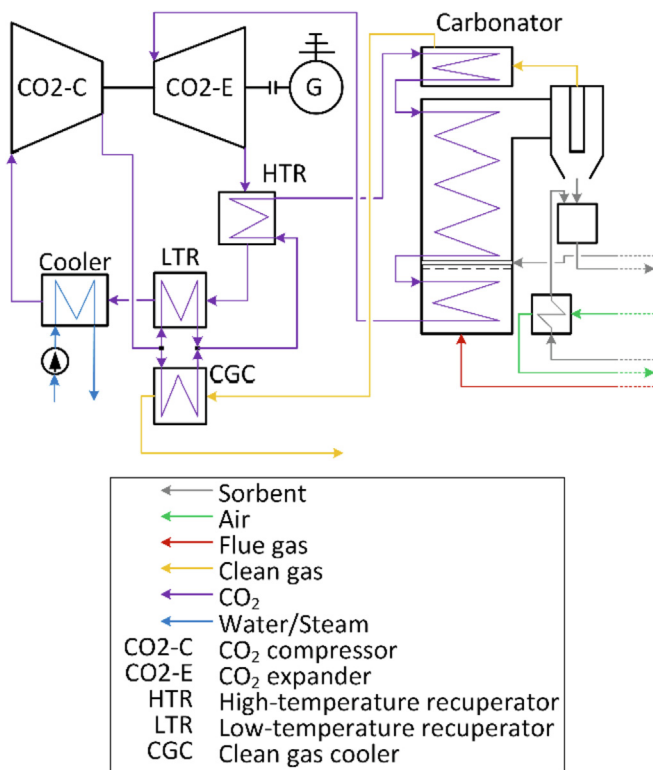


Fig. 2. Scheme of reference case: CaLC with steam cycle.

**Table 1**  
Initial process model assumptions for reference power plant (Hanak and Manovic, 2017a).

Subsystem	Parameter, Unit	Value
Combustor	Pressure drop, kPa	15
Calcliner	Pressure drop, kPa	15
	Calcination extent, -	0.95
	Recycled CO <sub>2</sub> fraction, -	0.2
Carbonator	Pressure drop, kPa	15
	Carbonation extent, -	0.7
Supercritical steam cycle	Feedwater heater terminal temperature difference, °C	10.0
	Feedwater heater minimum temperature approach, °C	2.8
	Isentropic efficiency of compressors, %	80.0
	Isentropic efficiency of high/intermediate/low-pressure steam turbine, %	83.8–84.5/88.0/88.0–92.7
	Isentropic efficiency of pumps, %	80.0
	Electrical efficiency of generator, %	98.5
	Mechanical efficiency of steam turbines, %	99.8
Heat exchanger network	Mechanical efficiency of compressors, %	99.6
	Sorbent cooler and heater minimum temperature approach, °C	25.0
	Air preheater minimum temperature approach, °C	10.0
	CO <sub>2</sub> preheater minimum temperature approach, °C	100.0
	Cold-/Hot-end temperature difference in the compressor intercooler, °C	15/30
	Cold-/Hot-end temperature difference in the last captured CO <sub>2</sub> cooler, °C	5/30
Auxiliary power assumptions	Intercoolers overall heat transfer coefficient, W/m <sup>2</sup> ·C	300
	Coal handling system specific power consumption, MJ/t <sub>coal</sub>	8.2
	Sorbent handling system specific power consumption, MJ/t <sub>sorbent</sub>	52.4
	Ash and used sorbent handling system specific power consumption, MJ/t <sub>ash/sorbent</sub>	31.2
	Cooling tower fan specific consumption, MJ/t <sub>cooling water</sub>	0.17



**Fig. 3.** Scheme of the CaLC s-CO<sub>2</sub> case.

an isentropic efficiency of 93%. After expansion to 7.4 MPa, the working fluid is cooled in two recuperators (HTR and LTR) and in the cooler to 31.25 °C, before it is compressed back to 20 MPa in the compressor with an isentropic efficiency of 85%. The mechanical efficiency of the compressor and expander is assumed to be 99%. Other assumptions and design specifications for the s-CO<sub>2</sub> cycle are

presented in Table 2.

### 3. Framework for techno-economic assessment

#### 3.1. Thermodynamic performance assessment

The thermodynamic assessment used in this paper follows the same approach as presented in previous work (Hanak and Manovic, 2016, 2017a, 2018). The most important thermodynamic performance indicator is the net efficiency of the entire system. As defined in Eq. (3), this quantity depends on the gross power output ( $P_G$ ), total auxiliary power requirement ( $\sum P_{AUX}$ ), fuel flow rate ( $\dot{m}_F$ ), and HHV of fuel.

$$\eta_N = \frac{P_G - \sum P_{AUX}}{\dot{m}_F \cdot HHV} \quad (3)$$

The gross power output of CaLC is the electric power output of the generator linked with the mechanical shaft in the conventional steam cycle or the s-CO<sub>2</sub> cycle. The total auxiliary power requirement (Eq. (4)), on the other hand, is the sum of all auxiliary power requirements of CaLC ( $P_{CaLC}$ ), CCT ( $P_{CCT}$ ) and the conventional steam or s-CO<sub>2</sub> cycle ( $P_{Cycle}$ ).

$$\sum P_{AUX} = P_{CaLC} + P_{CCT} + P_{Cycle} \quad (4)$$

In CaLC, the auxiliary power requirement arises from the power requirements of coal, sorbent, ash, and spent sorbent handling systems, coal pulveriser, primary air fan, cooling air fan, and CO<sub>2</sub> recirculation fan. The power requirements of the CO<sub>2</sub> compressor and CO<sub>2</sub> pump are included in the auxiliary power requirement of the CCT. In the s-CO<sub>2</sub> cycle, the auxiliary power requirement includes only the power requirement of the cooling water pump and the cooling tower fan. In the conventional steam cycle, the additional condensate and main cycle pumps are included.

For low-CO<sub>2</sub>-emission power plants, specific CO<sub>2</sub> emissions are considered as a key parameter to determine their environmental performance. This parameter relates the amount of CO<sub>2</sub> emitted to



**Table 2**Initial process model assumptions for CaLC power plant with s-CO<sub>2</sub> cycle.

Parameter, Unit	Value
Relative pressure loss in:	
cold side of LTR, HTR and CGC2 heat exchangers, %	0.5
hot side of LTR and HTR heat exchangers, %	1.0
cold side of carbonator clean gas cooler, %	0.3
cold side of carbonator reaction zone heat exchanger, %	0.5
cold side of carbonator flue gas cooler, %	0.2
hot side of cooler, %	1.0
Electric generator efficiency, %	98.5
Cooling water parameters at the inlet to the water pump, °C/MPa	20/0.1
Water pump pressure ratio, -	2.0
Water temperature at the outlet of cycle medium cooler, °C	25
HTR and LTR overall heat transfer coefficient, W/m <sup>2</sup> ·°C (Marchionni et al., 2017)	1700
Cooler overall heat transfer coefficient, W/m <sup>2</sup> ·°C (Marchionni et al., 2017)	2900

the net power output of the entire system.

### 3.2. Economic performance assessment

As indicated above, the method employed in previous research to perform the economic assessment was largely based on the levelised approach to estimating cost of electricity (Hanak et al., 2018a; Hanak and Manovic, 2017a, 2018). The method takes into account many aspects associated with the financial operation of the power plant, such as investment, fuel, operating and maintenance costs, and discount rate (Abanades et al., 2007; Zhao et al., 2013). However, this method does not consider important factors such as tax, depreciation, investment funding structure (loan, equity, subsidy), and interest rates. Additionally, only the investment costs are discounted within this method. Thus, it is pertinent to use methods that better reflect the actual economic performance, such as the NPV method, where the annual cash flows are discounted and then summarised (Kotowicz and Michalski, 2016, 2015; Ma et al., 2017, 2015; Pike et al., 2015). This work uses the break-even point (BEP) to assess the economic performance of the considered cases. This approach is based on the NPV method that is commonly applied in assessment of engineering systems (Hanak and Manovic, 2018; Kotowicz and Michalski, 2015, 2016, Ma et al., 2015, 2017). The NPV (Eq. (5)) is the sum of the discounted annual cash flows ( $CF_t$ ) throughout the system lifetime associated with investment. Thus, it depends additionally on the current building/operation year ( $t$ ), discount rate ( $r$ ), and total number of building and operation years ( $n$ ).

$$NPV = \sum_{t=1}^{t=n} \frac{CF_t}{(1+r)^t} \quad (5)$$

In the BEP case, the value of the selected economic performance indicator for which the NPV is zero is estimated. Such an approach allows estimating the minimum figure for the parameters used in the NPV method. The values of such parameters are usually challenging to estimate over the considered time frame. For the cases considered in this work, there are two key economic performance indicators that need to be estimated: the electricity price and carbon tax. The value of the latter parameter has been increasing over the past 12 months (6/29/2017 – ~5 €/t<sub>CO<sub>2</sub></sub>; 1/25/2018 – ~9 €/t<sub>CO<sub>2</sub></sub>; 6/14/2018 – ~15 €/t<sub>CO<sub>2</sub></sub>) (Business Insider, 2018). Thus, in this work the break-even price of electricity ( $BEP_{el}$ ) is calculated and the carbon tax is initially assumed to be 0. To evaluate the effect of the latter parameter on  $BEP_{el}$ , a parametric study is conducted.

Moreover, the economic performance assessment is carried out using a discount rate of 6%, which is the minimum recommended value in Steinbach and Staniaszek (2015). The annual cash flows (Eq. (6)) depend on the annual investment cost ( $C_{Inv}$ ), income from

electricity sales ( $I_{El}$ ), operating cost ( $C_{Op}$ ), income tax ( $C_{Tax}$ ), depreciation ( $D$ ) and salvage value ( $I_{Sa}$ ), the last of which appears only in the last operational year.

$$CF_t = [-C_{Inv} + I_{El} - (C_{Op} + C_{Tax}) + D + I_{Sa}]_t \quad (6)$$

The investment cost appears only during the building period, and its annual allocation depends on the assumed annual fraction of the total investment cost of the system. In this work, it is assumed that the building period is divided into four years. The method of total investment cost estimation is presented in detail in Section 3.3.

The income from electricity sales is calculated using the estimated break-even electricity price and the amount of electricity produced in the current operating year. The operating costs are the sum of fixed and variable costs. The fixed costs include the repair cost (from 0.5 to 2.5% of the total investment costs), depreciation (spread over 10 years), insurance cost (equal to 0.2% of the total investment costs) and maintenance cost. To estimate the maintenance cost, it was assumed that the annual average income of an employee is 43 900 €. This figure is based on the 2011 statistical data for industry and services employees in the UK (Eurostat, 2018) and the inflation rate. The employment rate is assumed to be 0.2 person/MW<sub>el, gross</sub> (EDF Energy, 2018). The variable costs include fuel cost, CO<sub>2</sub> emission cost (depending on the carbon tax), steam cycle exploitation cost, and CaLC unit exploitation cost. The fuel cost is calculated based on the unit cost of coal of 58.75 €/t (EURACOAL, 2017). The steam cycle exploitation cost depends on annual operating time of the system ( $\tau$ ), flow rate of make-up water ( $\dot{V}_{H2O}$ ), chemical flow rate for water treatment ( $\dot{m}_{Chem}$ ), unit price of the water ( $c_{H2O}$ ), and unit price of the chemical ( $c_{Chem}$ ), as shown in Eq. (7). It was assumed that the leakage of the working medium in the s-CO<sub>2</sub> cycle will be replenished using the captured CO<sub>2</sub>. The costs of replenishment in such a cycle are the highest of all exploitation costs. However, due to the simplification of calculations, it was assumed that the exploitation costs of the s-CO<sub>2</sub> cycle are equal to steam cycle exploitation costs.

$$C_{SC,ex} = \tau \cdot (\dot{V}_{H2O} \cdot c_{H2O} + \dot{m}_{Chem} \cdot c_{Chem}) \quad (7)$$

The CaLC unit exploitation costs depend on annual operating time of the system ( $\tau$ ), the fresh sorbent make-up flow rate ( $\dot{m}_{CaCO3}$ ), disposed ash flow rate ( $\dot{m}_{D,Ash}$ ), disposed sorbent flow rate ( $\dot{m}_{D,Sorb}$ ), unit price of fresh sorbent ( $c_{CaCO3}$ ), and unit cost of disposal ( $c_D$ ), as shown in Eq. (8).

$$C_{CaLC,ex} = \tau \cdot [\dot{m}_{CaCO3} \cdot c_{CaCO3} + (\dot{m}_{D,Ash} + \dot{m}_{D,Sorb}) \cdot c_D] \quad (8)$$

The annual operating time of the system is calculated according to the capacity factor, which is assumed to be 85% (Fout et al., 2015).

The income tax depends on the income from electricity sales ( $I_{El}$ ), operating cost ( $C_{Op}$ ), interest payable ( $C_{Int}$ ) and income tax rate ( $r_{Tax}$ ), as shown in Eq. (9).

$$C_{Tax} = [I_{El} - (C_{Op} + C_{Int})] \cdot r_{Tax} \quad (9)$$

The income tax rate is assumed at the level of the UK corporate tax rate of 19%. For the calculation of the interest charge, it is assumed that 80% of the total investment costs are covered by a commercial loan with interest rate of 6% and the loan repayment time of 15 years. Finally, the salvage value is considered as 20% of the total investment costs.

### 3.3. Investment cost estimation

An accurate estimation of the total as-spent investment cost of power generation systems is challenging, even in the case of mature conventional coal-fired power plants (Koornneef et al., 2008; Kotowicz and Michalski, 2015). Implementation of cutting-edge technology into power generation systems makes this task even harder. In this work, the total as-spent investment costs are defined in Eq. (10) and depend on labour cost indicator ( $i_{LC}$ ), engineering and project cost indicator ( $i_{E\&PC}$ ), total as-spent cost (TASC) multiplier ( $i_{TASC}$ ), land and owner's cost ( $C_{L\&O}$ ), as well as investment costs of CaLC ( $C_{CaLC}$ ), power generation cycle (conventional steam or s-CO<sub>2</sub> cycle) ( $C_{Cycle}$ ), and CCT ( $C_{CCT}$ ).

$$C_{Inv} = i_{TASC} \cdot [(1 + i_{LC} + i_{E\&PC}) \cdot (C_{CaLC} + C_{Cycle} + C_{CCT}) + C_{L\&O}] \quad (10)$$

Eq. (10) was developed based on the research presented in Fout et al. (2015). After critical evaluation of the cost estimation results for all cases reported in that source, it was assumed that the labour cost indicator, engineering and project cost indicator, and TASC multiplier are equal to 0.5, 0.35 and 1.13, respectively. More attention was dedicated to Case B12A in Fout et al. (2015) because of the similarity of the steam cycle parameters compared to those used in the reference case considered in this work. Based on this, it was assumed that the conventional steam cycle investment cost is 244 417 kUS\$. Considering the inflation rate (2015–2017) and exchange rate of 1.177 US\$/€ (Bank of England, 2018), this figure becomes 214 443 k€. Additionally, it was assumed that the value of land and owner's cost is 198 940 k€ (234 185 kUS\$ in 2015), according to the same case study.

The investment cost of CaLC was estimated using the bottom-up approach, based on the capital cost of components, as presented in Eq. (11). Thus, this figure depends on the piping and integration costs indicator ( $i_{P\&C} = 5\%$ ), as well as the capital costs of calciner ( $C_{Cal}$ ), carbonator ( $C_{Car}$ ), fuel preparation system ( $C_{FP}$ ), three fans ( $\Sigma C_{Fan}$ ) and six heat exchangers ( $\Sigma C_{HE}$ ).

$$C_{CaLC} = (1 + i_{P\&C}) \cdot (C_{Cal} + C_{Car} + C_{FP} + \Sigma C_{Fan} + \Sigma C_{HE}) \quad (11)$$

Estimation of the calciner and carbonator cost was based on the heat flux ( $\dot{Q}_{Cal}$  and  $\dot{Q}_{Car}$ , respectively) that was used as the quantity affecting the scale of the reactors, using Eq. (12) and Eq. (13), respectively.

$$C_{Cal} = c_{Cal} \cdot \dot{Q}_{Cal}^{0.67} \quad (12)$$

$$C_{Car} = c_{Car} \cdot \dot{Q}_{Car}^{0.67} \quad (13)$$

The reactors used in the CaLC unit can be considered as a replacement of the boilers used in conventional coal-fired power plants. The calciner comprises elements of the radiation part of the

conventional boilers, such as combustion chamber and radiative heat exchanger, while the carbonator comprises elements of the convective part of the conventional boilers, such as economisers, evaporator and superheaters. Components that are not present in the conventional boilers are mainly carbonator and calciner reaction zones. Thus, it was assumed that the heat flux scaling exponent is the same as in conventional boilers, and amounts to 0.67 (Fout et al., 2015). Then, based on the study by Criado et al. (2017), the unit prices of the calciner and carbonator were determined ( $c_{Cal} = 13\,140\text{ €/kW}^{0.67}$ ;  $c_{Car} = 16\,591\text{ €/kW}^{0.67}$ ). Similarly, the investment cost of the fuel preparation system was calculated (Eq. (14)), with the difference that the fuel flow rate ( $\dot{m}_F$ ) was used as the scaling factor instead of the heat flux. The fuel flow rate scaling exponent of 0.24 and unit price of the fuel preparation system ( $c_{FP}$ ) of 14 158 479 €/kg/s<sup>0.24</sup> were assumed, according to Fout et al. (2015).

$$C_{FP} = c_{FP} \cdot \dot{m}_F^{0.24} \quad (14)$$

The fan cost estimation in Eq. (15) took into account the break power of the fan ( $P_{Fan}$ ), as presented in the current literature (Hanak and Manovic, 2018; Lee et al., 2014; Shirazi et al., 2012). The values of constants in Eqs. (15)–(19) and (23)–(25) were adapted to represent the capital cost in 2017€, where appropriate. The average (Oct.–Dec. 2017) exchange rate of 1.127 €/£ (Bank of England, 2018) was assumed.

$$C_{Fan} = 103193 \cdot \left( \frac{P_{Fan}}{445} \right)^{0.67} [\text{€}] \quad (15)$$

To estimate the price of the heat exchangers, Eq. (16) considered both the heat exchanger surface area ( $A_{HE}$ ) and the operating pressure of such devices ( $p_{HE}$ , bar) (Gabbriellini and Singh, 2005).

$$C_{HE} = 2546.9 \cdot A_{HE}^{0.67} \cdot p_{HE}^{0.28} [\text{€}] \quad (16)$$

The estimation of the investment cost of the s-CO<sub>2</sub> unit is more difficult than estimation of the cost of the steam cycle, as there is no reliable source of data. Thus, for this work the estimation method of the investment cost of the s-CO<sub>2</sub> unit, presented in Eq. (17), was developed. The quantity depends on the piping and integration costs indicator ( $i_{P\&C}$ ), as well as the costs of the CO<sub>2</sub> compressor ( $C_C$ ), CO<sub>2</sub> expander ( $C_E$ ), electric generator ( $C_{EG}$ ), three heat exchangers ( $\Sigma C_{HE}$ ) and cooling tower ( $C_{CT}$ ).

$$C_{Cycle, CO_2} = (1 + i_{P\&C}) \cdot (C_C + C_E + \Sigma C_{HE} + C_{EG} + C_{CT}) \quad (17)$$

The most important components of such a cycle are the supercritical CO<sub>2</sub> compressor and expander. To estimate investment costs of both elements, the methodology presented in Benjelloun et al. (2012) was used. The investment cost of the CO<sub>2</sub> compressor (Eq. (18)) depends on the equivalent mass flow rate of air ( $\dot{m}_{AE, Com}$ ), compressor isentropic efficiency ( $\eta_{i, Com}$ ), compressor inlet pressure ( $p_{in}$ ) and equivalent air outlet pressure ( $p_{AE, out}$ ).

$$C_C = \dot{m}_{AE, Com} \cdot c \cdot \frac{47.1}{1 - \eta_{i, C}} \cdot \frac{p_{AE, out}}{p_{in}} \cdot \ln \left( \frac{p_{AE, out}}{p_{in}} \right) \quad (18)$$

On the other hand, the investment cost of the CO<sub>2</sub> expander depends (Eq. (19)) on the equivalent mass flow rate of air ( $\dot{m}_{AE, Com}$ ), expander isentropic efficiency ( $\eta_{i, Exp}$ ), expander inlet pressure ( $p_{in}$ ) and equivalent air outlet pressure ( $p_{AE, out}$ ).

$$C_E = \dot{m}_{AE,E} \cdot \frac{392.2}{1 - \eta_{i,E}} \cdot \frac{p_{in}}{p_{AE,out}} \cdot \ln\left(\frac{p_{in}}{p_{AE,out}}\right) \cdot [1 + \exp(0.036 \cdot T_{in} - 65.66)] \quad (19)$$

To calculate the equivalent mass flow rate of air, in both cases (Eq. (18) and (19)), the volumetric flow rate of air and CO<sub>2</sub> at the inlet to the compressor and expander were assumed to be the same. Thus, the ratio of air ( $\rho_{in,Air}$ ) and CO<sub>2</sub> ( $\rho_{in,CO_2}$ ) density at the inlets was used, as presented in Eq. (20).

$$\dot{m}_{AE,C/E} = \dot{m}_{CO_2,C/E} \cdot \frac{\rho_{in,Air}}{\rho_{in,CO_2}} \quad (20)$$

In the case of equivalent air outlet pressure in the compressor and expander, the outlet volumetric flow rates of CO<sub>2</sub> and air were assumed to be the same. Thus, first the outlet density of the air was calculated using Eq. (21).

$$\rho_{out,Air} = \frac{\dot{m}_{AE,C/E}}{\dot{m}_{CO_2,C/E}} \cdot \rho_{out,CO_2} \quad (21)$$

Next, the proper equivalent air outlet pressures are determined iteratively with the aim of getting the proper values of air density. It is worth noting that in all calculations associated with Eqs. (20) and (21), the real gas database (CoolProp) was used (Massachusetts Institute of Technology, 2018). Importantly, the constant (392.2) in Eq. (19) was derived based on the results presented in the current literature (Criado et al., 2017; Gabbrielli and Singh, 2005). The total cost of HTR, LTR and cooler was estimated using Eq. (16). The electric generator cost is estimated using Eq. (22) that considers the gross power output of the generator ( $P_G$ ) as the scaling factor (Hanak and Manovic, 2018).

$$C_{EG} = 84.5 \cdot P_G^{0.95} [\text{€}] \quad (22)$$

The cost of the cooling tower was also considered. As presented in Eq. (23), the quantity depends on the cooler heat duty ( $\dot{Q}_{Cooler}$ ). The constant value of 32.3 was determined using the results presented in Fout et al. (2015).

$$C_{CT} = 32.3 \cdot \dot{Q}_{Cooler} [\text{€}] \quad (23)$$

The last component of both cases considered in this work is the CCT (Eq. (24)). The investment cost of this unit depends on the piping and integration costs indicator ( $i_{P\&C}$ ) and the costs of CO<sub>2</sub> compressor ( $C_C$ ), CO<sub>2</sub> expander ( $C_E$ ) and nine CO<sub>2</sub> intercoolers ( $\Sigma C_{HE}$ ).

$$C_{CCT} = (1 + i_{P\&C}) \cdot (C_C + C_P + \Sigma C_{HE}) \quad (24)$$

The compressor cost is calculated the same way as the compressor in the s-CO<sub>2</sub> cycle (Eq. (18)). The CO<sub>2</sub> intercoolers cost was estimated according to Eq. (16). The CO<sub>2</sub> pump cost was estimated using Eq. (25) (Gabbrielli and Singh, 2005) that takes the brake power ( $P_P$ ) and isentropic efficiency ( $\eta_{i,P}$ ) of such pump into consideration.

$$C_P = 3531.4 \cdot P_P^{0.71} \cdot \left[ 1 + \left( \frac{1 - 0.8}{1 - \eta_{i,P}} \right)^3 \right] \quad (25)$$

## 4. Techno-economic assessment

### 4.1. Results and discussion

After computations made with the reference case, the auxiliary power requirement of the reference power plant was determined to be 85.9 MW. The exact distribution of auxiliary power requirement is presented in Fig. 4. The largest part of this quantity is the power requirement of the CCT (52.3%). The reference power plant was characterised with a net power output of 508.3 MW, net efficiency of 35% and specific CO<sub>2</sub> emission of 101.9 kg/MWh. The gross power output of the s-CO<sub>2</sub> case is 508 MW; thus, it is smaller than in the reference power plant by 86.2 MW. The auxiliary power requirement is smaller in this case by 13.7 MW. According to results presented in Fig. 4, the power requirement of the CCT is still the largest part of this quantity (62.3%). Finally, the net power output of the s-CO<sub>2</sub> case (435.8 MW) is smaller than that of the reference power plant by 72.5 MW. Therefore, the net efficiency is lower than for the reference case by 5% points. The specific emission of CO<sub>2</sub> (118.9 kg/MWh), related with the efficiency, is higher by 17 kg/MWh.

The economic results show that the total investment cost of the reference case is 1546.4 M€<sub>2017</sub>, while it is lower for the s-CO<sub>2</sub> case by 186 M€ (12%). The distribution of equipment and material costs of the power plant components are presented in Fig. 5. In both cases, the main part of the equipment cost is the CaLC cost (Reference case – 62.2%; s-CO<sub>2</sub> case – 72.7%). It is worth noting that the decrease in power plant cost in the s-CO<sub>2</sub> case is associated with the 42.1%-decrease of the power cycle cost compared to the reference case. The break-even price of electricity calculated for the reference case is 83.51 €/MWh. The same quantity for the s-CO<sub>2</sub> case is 91.41 €/MWh.

In conclusion, the considered configuration of the s-CO<sub>2</sub> cycle is less efficient thermodynamically than the reference power plant. Additionally, despite the lower total as-spent investment cost, it has a higher break-even price of electricity than that of the reference power plant (by 7.9 €/MWh).

### 4.2. Parametric study

In order to improve the techno-economic parameters of the s-CO<sub>2</sub> case, revision of the s-CO<sub>2</sub> cycle operating conditions needs to be undertaken. Thus, the parametric study of the s-CO<sub>2</sub> case techno-economic algorithm was prepared. Two CaLC unit parameters, five s-CO<sub>2</sub> unit parameters and one economic parameter (the carbon tax, mentioned in Section 3.2) were selected for the

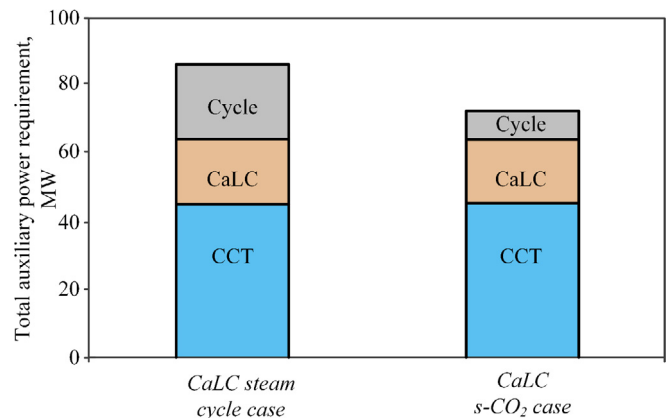


Fig. 4. Auxiliary power distribution.

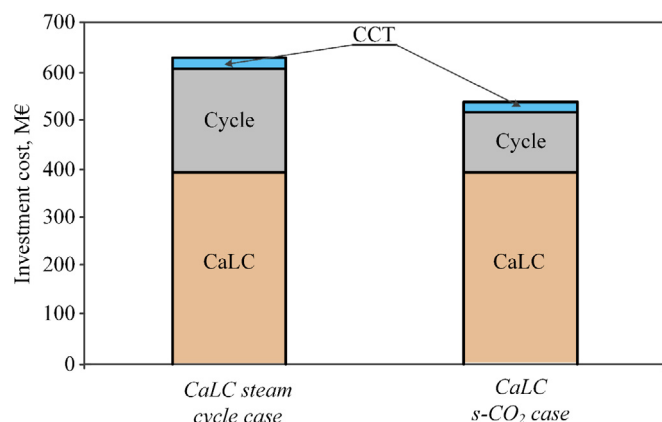


Fig. 5. Equipment and material cost composition.

parametric study. The chosen quantities along with their minimal and maximal values are presented in Table 3. For the calculations, both limiting values and three additional values between these were used. The maximal live CO<sub>2</sub> temperature is the result of the assumption that the minimal cold-end flue gas cooler temperature difference is 10 °C. The minimal pressure at the outlet of the compressor is the result of the mentioned temperature difference and additionally the range of live CO<sub>2</sub> temperature.

The parametric study of the CaLC parameters on the net efficiency of the power plant and break-even price of electricity are presented in Fig. 6. The best thermodynamic and economic results are obtained for the smallest values of both parameters. The impact of the relative make-up of sorbent change is more than 11 times higher on the thermodynamic factor and more than 30 times on the economic factor, even when the relative change of oxygen content is higher. The results are changing by 2% points (for net efficiency) and 18.1 €/MWh (for break-even price of electricity) compared to 0.18% points and 0.6 €/MWh in the case of oxygen concentration in the flue gas.

The two parameters of the s-CO<sub>2</sub> unit that should have the greatest impact on the techno-economic performance are the live CO<sub>2</sub> temperature and the compressor outlet pressure. Both parameters should be treated in a similar way as in the conventional steam cycle, because the optimal pressure can be different for different temperatures. Thus, the parametric studies of both parameters on the net efficiency of the power plant and the break-even price of electricity are presented in Fig. 7 and Fig. 8, respectively. The thermodynamic results show that the highest net efficiency occurs for the highest considered temperature and pressure. After a deeper analysis of the shape of the curves in Fig. 7, it can be seen that it is possible to find an optimal pressure for the considered temperatures, but pressure values must be much higher than those considered in this paper.

Fig. 8 indicates that the break-even price of electricity decreases

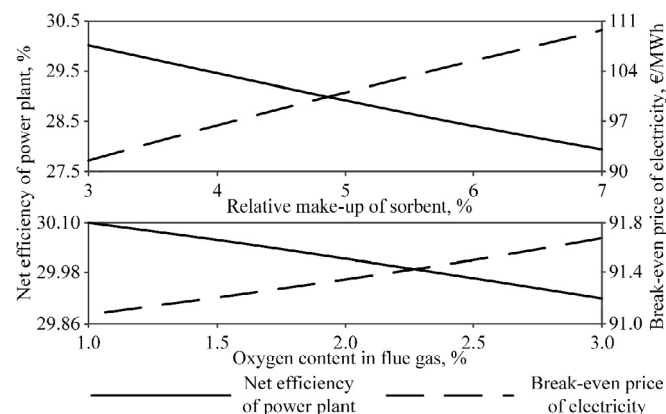


Fig. 6. CaLC unit parametric study results.

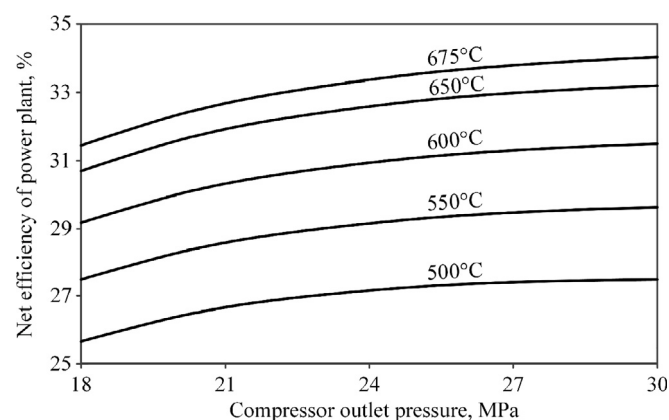


Fig. 7. Influence of live CO<sub>2</sub> temperature and the compressor outlet pressure on the net efficiency.

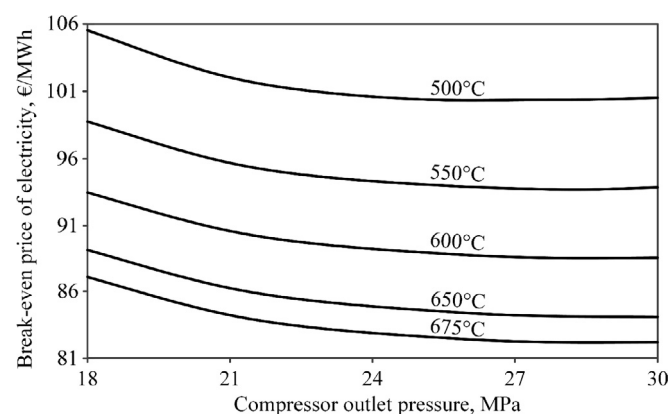


Fig. 8. Influence of live CO<sub>2</sub> temperature and the compressor outlet pressure on the break-even price of electricity.

Table 3  
Parametric study assumptions.

Parameter, Unit	Minimal value	Maximal value
Oxygen concentration in the flue gas, %	1.0	3.0
Relative make-up of sorbent, %	3.0	7.0
Live CO <sub>2</sub> temperature, °C	500	675
Compressor outlet pressure, MPa	18	30
HTR cold-end temperature difference, K	5	15
LTR cold-end temperature difference, K	5	15
LTR hot-end temperature difference, K	5	15
Carbon tax, €/t	0	100

as the live CO<sub>2</sub> temperature increases. The results for compressor pressure ratio show that there are optimal pressures of 27 MPa and 28.5 MPa for temperatures 500 °C and 550 °C, respectively. For the remaining temperatures, the optimal value is above the considered range of pressures.

The parametric study results for the other s-CO<sub>2</sub> parameters on the net efficiency and break-even price of electricity are presented in Fig. 9. Two of the parameters, the temperature difference at the cold end of the HTR and hot end of the LTR, have no impact on the



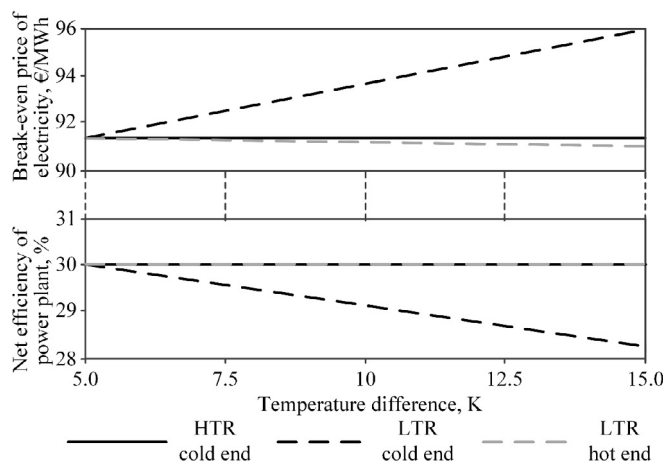


Fig. 9. Parametric study results of temperature differences in s-CO<sub>2</sub> cycle.

net efficiency of the power plant. The break-even price of electricity is marginally changed by 0.05 €/MWh for the first quantity, with the lowest value occurring for a temperature difference of 7.5 K. The temperature difference at the hot end of the LTR had a greater impact on the break-even price of electricity, with the value reduced by 0.34 €/MWh for an increase of the temperature difference from 5 K to 15 K. The greatest impact on the net efficiency of the power plant relates to the temperature difference at the cold end of the LTR. The efficiency decreased by 1.74% points with an increase of the temperature difference from 5 K to 15 K. These results coincide with those anticipated. The increased temperature difference at the cold end of the LTR caused a decrease of the heat flux transferred in the LTR and, as a result, additional heat flux was needed from elsewhere. However, due to the assumptions made, increasing the heat transferred from the CaLC unit is not possible, so the live flow rate of CO<sub>2</sub> must decrease. Finally, the gross power output of the power plant decreased. The break-even price of electricity changed value by 4.61 €/MWh during the parametric study of the temperature difference at the cold end of the LTR. This outcome is the result of three changes: decrease of the net efficiency, decrease of the LTR cost, and increase of the cooler and cooling tower costs.

Taking the parametric study results into account, up to this point, new revised assumptions were made. For both cases studied the best economic performance was reported for the oxygen content in flue gas of 1%, thus this value was assumed. As a result, the reference power plant net efficiency was increased by 0.1% point (to 35.1%), the specific CO<sub>2</sub> emission decreased by 0.4 kg/MWh (to 101.5 kg/MWh), the total investment cost decreased by 13.2 M€ (to 1533.2 M€) and the break-even price of electricity decreased by 0.66 €/MWh (to 82.85 €/MWh). Additionally, for the s-CO<sub>2</sub> power plant the revised values, according to economic results, the live CO<sub>2</sub> temperature (675 °C), the compressor pressure (30 MPa) and the temperature difference at the cold end of the HTR (7.5 K), were assumed. The revised values of s-CO<sub>2</sub> parameters increased the net power output of the power plant by 60.5 MW. As a result, the net efficiency of the power plant increased to 34.2% (by 4.2% points) and the specific CO<sub>2</sub> emission was reduced by 14.5 gCO<sub>2</sub>/kWh. Still, the net efficiency of the s-CO<sub>2</sub> case is lower than for the reference power plant (by 0.9% point). The economic results show a decrease of the break-even price of electricity by 9.38 €/MWh. Finally, the value is slightly lower than for the reference case by 0.81 €/MWh. It should be noted that the techno-economic performance of the proposed concepts can be further improved through optimisation of the s-CO<sub>2</sub> cycle structure, which is out of the scope for this study.

The economic performance considering the LCOE of the reference case was previously analysed by Hanak and Manovic (2017a), which showed that the specific capital cost and LCOE are 1837.1 €/kW<sub>gross</sub> and 64.6 €/MWh, respectively. Using the methodologies presented in this paper, the specific capital cost is higher by 40% (2573.5 €/kW<sub>gross</sub>). It needs to be highlighted that both the analysis presented in this work and analysis made by Hanak and Manovic (2017a) use the same reference results from Fout et al. (2015) for material and labour costs validation. Thus, the difference in the specific capital cost is mainly caused by adoption of the total as-spent investment costs calculation method presented as Eq. (10) and based on results from Fout et al. (2015). The break-even price of electricity is higher by 18.9 €/MWh than LCOE calculated for the same structure of CaLC power plant, raising the value by 29.3%. For the same TASC of power plant the BEP<sub>el</sub> is higher by 6.78 €/MWh than the LCOE, thus almost 67% of the increase is associated with the investment cost increase.

The economic sensitivity analysis was performed for 13 selected parameters, which were varied by ±15% of their initial value. The results for revised assumptions of both cases are presented in Fig. 10 in the order of decreasing influence. The last five parameters changed the break-even electricity price by less than ±0.5%.

The results of the carbon tax parametric study for the reference and s-CO<sub>2</sub> cases are presented in Fig. 11. Computations were made for initial and revised assumptions. In the reference case the change of the allowance cost increased the break-even price of electricity by 10.2 €/MWh for nominal and revised assumptions. The curves representing results for initial and revised assumptions in this case are very close to each other, because the assumptions only differ with the oxygen content in the flue gas. In the s-CO<sub>2</sub> case the

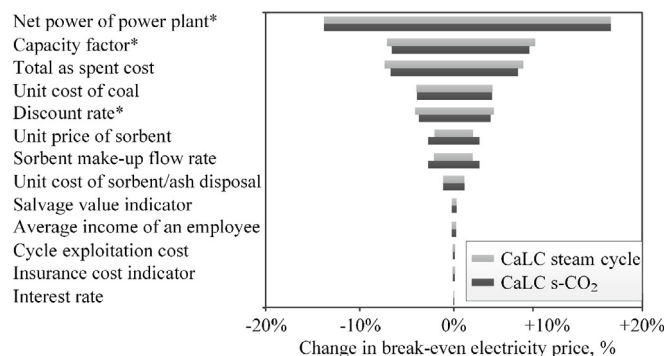


Fig. 10. Economic sensitivity analysis results (\*nonlinear characteristic).

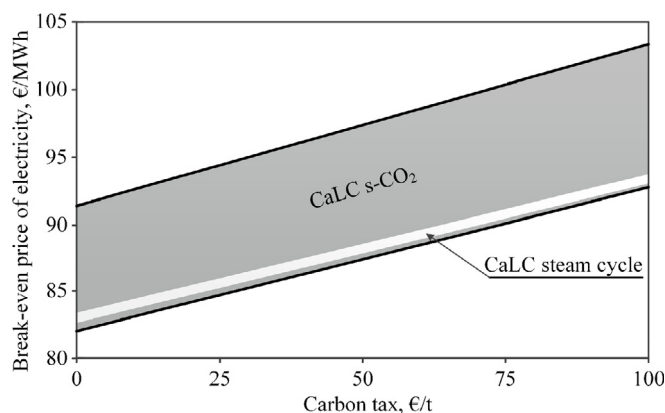


Fig. 11. Parametric study results of carbon tax.

**Table 4**

Benchmark of CaLC techno-economic performance with other power generation technologies.

Parameter, Unit	Coal-fired power plant without CCS	Amine retrofit	CaLretrofit	CaLC steam cycle	CaLCs-CO <sub>2</sub>
Total as spent cost, M€ <sub>2017</sub>	1373.5	1903.6	2746.0	1533.2	1421.3
Net power, MW	552.6	416.2	799.9	510.3	496.3
Net efficiency, %	38.0	28.7	30.6	35.1	34.2
Unit CO <sub>2</sub> emission, kg/MWh	796.8	105.8	98.9	101.5	104.4
Break-even electricity price, €/MWh	59.63	96.43	86.00	82.85	82.04
Net efficiency penalty, % points	–	9.4	7.4	2.9	3.9
Break-even electricity price penalty, €/MWh	–	36.80	26.38	23.22	22.41

increase is higher (11.9 €/MWh) for the initial assumptions. For the revised assumptions the increase is close to that of the reference case (10.5 €/MWh).

To emphasise the advantages of the CaLC-based power plant, the conventional coal-fired power plant without CCS, coal-fired power plant retrofitted with amine scrubbing (amine retrofit) and coal-fired power plant retrofitted with CaL (CaL retrofit) are compared (Hanak et al., 2015b; Hanak and Manovic, 2017a) in Table 4. The TASC for the power plant without CCS is assumed to be the same as in the B12A case from Fout et al. (2015). The TASC for the amine retrofit is based on the B12B case from Fout et al. (2015) and was adjusted to represent the same fuel flow rate. Finally, to calculate the TASC of the CaL retrofit, the capital cost of an air separation unit (ASU) and CaL unit were added to the capital cost of the conventional coal-fired power plant without CCS. The capital cost of the ASU was calculated according to the methodology used by Hanak and Manovic (2018), while the CaL unit capital cost is calculated according to Eq. (11)–(16).

## 5. Conclusions

The purpose of this study was to use an economic analysis method that gave results closer to reality, compared to the previous approach taken by several authors (levelised cost of electricity – LCOE). This includes the total as-spent cost of the CaLC power plant estimation method, which takes the scale factor of equipment into account. The proposed scale factors are the main thermodynamic parameters of the individual devices and machines (such as carbonator heat load). It is worth noting that the CaLC unit and s-CO<sub>2</sub> cycle investment costs are calculated using an unconventional method. This allows changing the scale of those units over a wide range. The study proposed the use of the break-even price of electricity as an economic investment evaluation method for power plants based on the CaLC technology. This approach is based on the net present value method of economic analysis. The method is much more comprehensive than LCOE, as it takes into consideration cash flows during construction and operation years of the power plant. Additionally, the method includes economic quantities such as taxes, interest and depreciation. Finally, cash flows are discounted instead of only discounting investment costs (as in the LCOE method).

The economic method was then used as part of a techno-economic assessment of two variants of the CaLC power plant. The 594.2 MW<sub>el, gross</sub> low-CO<sub>2</sub>-emission power plant that is composed of a CaLC unit integrated with supercritical steam cycle was the first (reference) case. The second case was the 508 MW<sub>el, gross</sub> low-CO<sub>2</sub>-emission power plant which contains a supercritical CO<sub>2</sub> (s-CO<sub>2</sub>) cycle (instead of the steam cycle). The evaluation under the initial design basis has indicated that the reference case net efficiency of the power plant is higher by 5% points than for the s-CO<sub>2</sub> case. The associated break-even prices of electricity were 83.51 €/MWh and 91.41 €/MWh, respectively. The parametric study of the CaLC parameters showed that the relative make-up of sorbent

had a great impact on the economic and thermodynamic performance of the entire power plant. Thus, during the research and design period of such technology, considerable effort should be made to reduce this parameter to the lowest possible level. After revision of the design basis (of both cases) using the parametric study findings, the net efficiency difference was lowered to 0.9% point. The break-even price relationship was reversed, with the value for the reference case slightly higher (by 0.81 €/MWh) than for the s-CO<sub>2</sub> case. The analysed power plant cases have relatively low efficiency penalties (2.9% points – reference case; 3.8% points – s-CO<sub>2</sub> case) and lower BEP<sub>el</sub> compared to other CCS technologies. The parametric study of CO<sub>2</sub> tax additionally confirmed that the s-CO<sub>2</sub> case can be more economically viable. The value of CO<sub>2</sub> tax that will reduce the probability of such situation is much higher than the range considered. The conclusion from the techno-economic assessment is that further improvement is still possible using structural optimisation or by implementing other types of closed Brayton cycles using different working fluids.

## Acknowledgements

This publication is based on research conducted within the “Redefining power generation from carbonaceous fuels with carbonate looping combustion and gasification technologies” project funded by UK Engineering and Physical Sciences Research Council (EPSRC reference: EP/P034594/1). Data underlying this study can be accessed through the Cranfield University repository at <https://doi.org/10.17862/cranfield.rd.7700915>.

## References

- Abanades, J., Grasa, G., Alonso, M., Rodriguez, N., Anthony, E.J., Romeo, L.M., 2007. Cost structure of a postcombustion CO<sub>2</sub> capture system using CaO. *Environ. Sci. Technol.* 41, 5523–5527. <https://doi.org/10.1021/es070099a>.
- Abanades, J.C., Anthony, E.J., Wang, J., Oakey, J.E., 2005. Fluidized bed combustion systems integrating CO<sub>2</sub> capture with CaO. *Environ. Sci. Technol.* 39, 2861–2866. <https://doi.org/10.1021/es0496221>.
- Arias, B., Diego, M.E., Abanades, J.C., Lorenzo, M., Diaz, L., Martinez, D., Alvarez, J., Sánchez-Biezma, A., 2013. Demonstration of steady state CO<sub>2</sub> capture in a 1.7 MWth calcium looping pilot. *Int. J. Greenh. Gas Control* 18, 237–245. <https://doi.org/10.1016/j.ijggc.2013.07.014>.
- AspenTech, 2017. *Aspen Plus V10*.
- Bank of England, 2018. Bank of England Statistical Interactive Database | Main Page [WWW Document]. URL <http://www.bankofengland.co.uk/boeapps/iadb/NewInterMed.asp?Travel=NixIRx>, accessed 5.23.18.
- Benjelloun, M., Doulgeris, G., Singh, R., 2012. A method for techno-economic analysis of supercritical carbon dioxide cycles for new generation nuclear power plants. *Proc. Inst. Mech. Eng. Part A J. Power Energy* 226, 372–383. <https://doi.org/10.1177/0957650911429643>.
- Boot-Handford, M.E., Abanades, J.C., Anthony, E.J., Blunt, M.J., Brandani, S., Mac Dowell, N., Fernández, J.R., Ferrari, M.-C., Gross, R., Hallett, J.P., Haszeldine, R.S., Heptonstall, P., Lyngfelt, A., Makuch, Z., Mangano, E., Porter, R.T.J., Pourkashanian, M., Rochelle, G.T., Shah, N., Yao, J.G., Fennell, P.S., 2014. Carbon capture and storage update. *Energy Environ. Sci.* 7, 130–189. <https://doi.org/10.1039/C3EE42350F>.
- Business Insider, 2018. CO<sub>2</sub> European Emission Allowances PRICE Today | Price of CO<sub>2</sub> European Emission Allowances and Chart | Markets Insider [WWW Document]. URL <http://markets.businessinsider.com/commodities/co2-emissionsrechte>, accessed 6.29.18.
- Chang, M.-H.H., Chen, W.W.-C.C., Huang, C.-M.M., Liu, W.-H.H., Chou, Y.-C.C.,

- Chang, W.-C.C., Chen, W.W.-C.C., Cheng, J.Y., Huang, K.-E.E., Hsu, H.-W.W., 2014. Design and experimental testing of a 1.9 MWth calcium looping pilot plant. *Energy Procedia* 63, 2100–2108. <https://doi.org/10.1016/j.egypro.2014.11.226>.
- Cormos, A.-M., Cormos, C.-C., 2017. Techno-economic evaluations of post-combustion CO<sub>2</sub> capture from sub- and super-critical circulated fluidised bed combustion (CFBC) power plants. *Appl. Therm. Eng.* 127, 106–115. <https://doi.org/10.1016/j.applthermaleng.2017.08.009>.
- Cormos, C.C., 2016. Oxy-combustion of coal, lignite and biomass: a techno-economic analysis for a large scale Carbon Capture and Storage (CCS) project in Romania. *Fuel* 169, 50–57. <https://doi.org/10.1016/j.fuel.2015.12.005>.
- Cormos, C.C., 2014. Economic evaluations of coal-based combustion and gasification power plants with post-combustion CO<sub>2</sub> capture using calcium looping cycle. *Energy* 78, 665–673. <https://doi.org/10.1016/j.energy.2014.10.054>.
- Criado, Y.A., Arias, B., Abanades, J.C., 2017. Calcium looping CO<sub>2</sub> capture system for back-up power plants. *Energy Environ. Sci.* 10, 1994–2004. <https://doi.org/10.1039/C7EE01505D>.
- Dean, C.C., Blamey, J., Florin, N.H., Al-Jeboori, M.J., Fennell, P.S., 2011. The calcium looping cycle for CO<sub>2</sub> capture from power generation, cement manufacture and hydrogen production. *Chem. Eng. Res. Des.* 89, 836–855. <https://doi.org/10.1016/j.cherd.2010.10.013>.
- Department of Energy and Climate Change, 2012. CCS Roadmap. Supporting Deployment of Carbon Capture and Storage in the UK. URN 12D/016.
- EDF Energy, 2018. Cottam and West Burton | Power Stations | EDF Energy [WWW Document]. URL: <https://www.edfenergy.com/energy/power-stations/cottam-west-burton-a>. accessed 5.21.18.
- EURACOAL, 2017. EURACOAL Market Report 2/2017.
- Eurostat, 2018. Database - Eurostat [WWW Document]. URL: <http://ec.europa.eu/eurostat/data/database>. accessed 5.21.18.
- Fout, T., Zoelle, A., Keairns, D., Turner, M., Woods, M., Kuehn, N., Shah, V., Chou, V., Pinkerton, L., 2015. Cost and Performance Baseline for Fossil Energy Plants Volume 1a: Bituminous Coal (PC) and Natural Gas to Electricity Revision 3. DOE/NETL 2010/1397.
- Gabbriellini, R., Singh, R., 2005. Economic and scenario analyses of new gas turbine combined cycles with No emissions of carbon dioxide. *J. Eng. Gas Turbines Power* 127, 531. <https://doi.org/10.1115/1.1850492>.
- Global CCS Institute, 2017. The Global Status of CCS, 2017.
- Hanak, D.P., Anthony, E.J., Manovic, V., 2015a. A review of developments in pilot-plant testing and modelling of calcium looping process for CO<sub>2</sub> capture from power generation systems. *Energy Environ. Sci.* 8, 2199–2249. <https://doi.org/10.1039/c5ee01228g>.
- Hanak, D.P., Biliyok, C., Anthony, E.J., Manovic, V., 2015b. Modelling and comparison of calcium looping and chemical solvent scrubbing retrofits for CO<sub>2</sub> capture from coal-fired power plant. *Int. J. Greenh. Gas Control* 42, 226–236. <https://doi.org/10.1016/j.ijggc.2015.08.003>.
- Hanak, D.P., Biliyok, C., Manovic, V., 2016. Calcium looping with inherent energy storage for decarbonisation of coal-fired power plant. *Energy Environ. Sci.* 9, 971–983. <https://doi.org/10.1039/c5ee02950c>.
- Hanak, D.P., Biliyok, C., Manovic, V., 2015c. Efficiency improvements for the coal-fired power plant retrofit with CO<sub>2</sub> capture plant using chilled ammonia process. *Appl. Energy* 151, 258–272. <https://doi.org/10.1016/j.apenergy.2015.04.059>.
- Hanak, D.P., Erans, M., Nabavi, S.A., Jeremias, M., Romeo, L.M., Manovic, V., 2018a. Technical and economic feasibility evaluation of calcium looping with no CO<sub>2</sub> recirculation. *Chem. Eng. J.* 335, 763–773. <https://doi.org/10.1016/j.cej.2017.11.022>.
- Hanak, D.P., Manovic, V., 2018. Combined heat and power generation with lime production for direct air capture. *Energy Convers. Manag.* 160, 455–466. <https://doi.org/10.1016/j.enconman.2018.01.037>.
- Hanak, D.P., Manovic, V., 2017a. Calcium looping combustion for high-efficiency low-emission power generation. *J. Clean. Prod.* 161, 245–255. <https://doi.org/10.1016/j.jclepro.2017.05.080>.
- Hanak, D.P., Manovic, V., 2017b. Economic feasibility of calcium looping under uncertainty. *Appl. Energy* 208, 691–702. <https://doi.org/10.1016/j.apenergy.2017.09.078>.
- Hanak, D.P., Manovic, V., 2016. Calcium looping with supercritical CO<sub>2</sub> cycle for decarbonisation of coal-fired power plant. *Energy* 102, 343–353. <https://doi.org/10.1016/j.energy.2016.02.079>.
- Hanak, D.P., Michalski, S., Manovic, V., 2018b. From post-combustion carbon capture to sorption-enhanced hydrogen production: a state-of-the-art review of carbonate looping process feasibility. *Energy Convers. Manag.* 177, 428–452. <https://doi.org/10.1016/j.enconman.2018.09.058>.
- Hanak, D.P., Powell, D., Manovic, V., 2017. Techno-economic analysis of oxy-combustion coal-fired power plant with cryogenic oxygen storage. *Appl. Energy* 191, 193–203. <https://doi.org/10.1016/j.apenergy.2017.01.049>.
- International Energy Agency, 2017a. Key World Energy Statistics.
- International Energy Agency, 2017b. Tracking Clean Energy Progress 2017.
- International Energy Agency, 2016. Energy, Climate Change and Environment 2016 Insights. <https://doi.org/10.1787/9789264266834-en>.
- Junk, M., Reitz, M., Ströhle, J., Epple, B., 2016. Technical and economical assessment of the indirectly heated carbonate looping process. *J. Energy Resour. Technol.* 138, 042210. <https://doi.org/10.1115/1.4033142>.
- Junk, M., Reitz, M., Ströhle, J., Epple, B., 2013. Thermodynamic evaluation and cold flow model testing of an indirectly heated carbonate looping process. *Chem. Eng. Technol.* 36, 1479–1487. <https://doi.org/10.1002/ceat.201300019>.
- Koornneef, J., van Keulen, T., Faaij, A., Turkenburg, W., 2008. Life cycle assessment of a pulverized coal power plant with post-combustion capture, transport and storage of CO<sub>2</sub>. *Int. J. Greenh. Gas Control* 2, 448–467. <https://doi.org/10.1016/j.ijggc.2008.06.008>.
- Kotowicz, J., Michalski, S., 2016. Thermodynamic and economic analysis of a supercritical and an ultracritical oxy-type power plant without and with waste heat recovery. *Appl. Energy* 179, 806–820. <https://doi.org/10.1016/j.apenergy.2016.07.013>.
- Kotowicz, J., Michalski, S., 2015. Influence of four-end HTM (high temperature membrane) parameters on the thermodynamic and economic characteristics of a supercritical power plant. *Energy* 81, 662–673. <https://doi.org/10.1016/j.energy.2015.01.010>.
- Le Moulec, Y., 2013. Conceptual study of a high efficiency coal-fired power plant with CO<sub>2</sub> capture using a supercritical CO<sub>2</sub> Brayton cycle. *Energy* 49, 32–46. <https://doi.org/10.1016/j.energy.2012.10.022>.
- Lee, Y.D., Ahn, K.Y., Morosuk, T., Tsatsaronis, G., 2014. Exergetic and exergoeconomic evaluation of a solid-oxide fuel-cell-based combined heat and power generation system. *Energy Convers. Manag.* 85, 154–164. <https://doi.org/10.1016/j.enconman.2014.05.066>.
- Li, Z.S., Cai, N.S., Croiset, E., 2008. Process analysis of CO<sub>2</sub> capture from flue gas using carbonation/calcination cycles. *AIChE J.* 54, 1912–1925. <https://doi.org/10.1002/aic.1486>.
- Ma, L.C., Castro-Dominguez, B., Kazantzis, N.K., Ma, Y.H., 2017. Economic performance evaluation of process system design flexibility options under uncertainty: the case of hydrogen production plants with integrated membrane technology and CO<sub>2</sub> capture. *Comput. Chem. Eng.* 99, 214–229. <https://doi.org/10.1016/j.compchemeng.2017.01.020>.
- Ma, L.C., Castro-Dominguez, B., Kazantzis, N.K., Ma, Y.H., 2015. Integration of membrane technology into hydrogen production plants with CO<sub>2</sub> capture: an economic performance assessment study. *Int. J. Greenh. Gas Control* 42, 424–438. <https://doi.org/10.1016/j.ijggc.2015.08.019>.
- Mac Dowell, N., Shah, N., 2015. The multi-period optimisation of an amine-based CO<sub>2</sub> capture process integrated with a super-critical coal-fired power station for flexible operation. *Comput. Chem. Eng.* 74, 169–183. <https://doi.org/10.1016/j.compchemeng.2015.01.006>.
- Mantripragada, H.C., Rubin, E.S., 2013. Calcium looping cycle for CO<sub>2</sub> capture - performance, cost and feasibility analysis. *Energy Procedia* 63, 2199–2206. <https://doi.org/10.1016/j.egypro.2014.11.239>.
- Marchionni, M., Bianchi, G., Tsamos, K.M., Tassou, S.A., 2017. Techno-economic comparison of different cycle architectures for high temperature waste heat to power conversion systems using CO<sub>2</sub> in supercritical phase. *Energy Procedia* 123, 305–312. <https://doi.org/10.1016/j.egypro.2017.07.253>.
- Massachusetts Institute of Technology, 2018. CoolProp.
- Park, J.H., Bae, S.W., Park, H.S., Cha, J.E., Kim, M.H., 2018. Transient analysis and validation with experimental data of supercritical CO<sub>2</sub> integral experiment loop by using MARS. *Energy* 147, 1030–1043. <https://doi.org/10.1016/j.energy.2017.12.092>.
- Perejón, A., Romeo, L.M., Lara, Y., Lisbona, P., Martínez, A., Valverde, J.M., 2016. The Calcium-Looping technology for CO<sub>2</sub> capture: on the important roles of energy integration and sorbent behavior. *Appl. Energy* 162, 787–807. <https://doi.org/10.1016/j.apenergy.2015.10.121>.
- Pike, R., Neale, B., Linsley, P., 2015. *Corporate Finance: Decisions & Strategies*, eighth ed. Pearson, Harlow, UK.
- Renner, M., 2014. Carbon prices and CCS investment: a comparative study between the European Union and China. *Energy Policy* 75, 327–340. <https://doi.org/10.1016/j.enpol.2014.09.026>.
- Rodríguez, N., Alonso, M., Abanades, J.C., 2010. Average activity of CaO particles in a calcium looping system. *Chem. Eng. J.* 156, 388–394. <https://doi.org/10.1016/j.cej.2009.10.055>.
- Romano, M.C., Spinelli, M., Campanari, S., Consonni, S., Cinti, G., Marchi, M., Borgarello, E., 2013. The Calcium looping process for low CO<sub>2</sub> emission cement and power. *Energy Procedia* 37, 7091–7099. <https://doi.org/10.1016/j.egypro.2013.06.645>.
- Romeo, L.M., Abanades, J.C., Escosa, J.M., Paño, J., Giménez, A., Sánchez-biezma, A., Ballesteros, J.C., 2008. Oxyfuel carbonation/calcination cycle for low cost CO<sub>2</sub> capture in existing power plants. *Energy Convers. Manag.* 49, 2809–2814. <https://doi.org/10.1016/j.enconman.2008.03.022>.
- Rubin, E.S., Davison, J.E., Herzog, H.J., 2015. The cost of CO<sub>2</sub> capture and storage. *Int. J. Greenh. Gas Control* 40, 378–400. <https://doi.org/10.1016/j.ijggc.2015.05.018>.
- Sánchez-Biezma, A., Paniagua, J., Diaz, L., Lorenzo, M., Alvarez, J., Martínez, D., Arias, B., Diego, M.E., Abanades, J.C., 2013. Testing postcombustion CO<sub>2</sub> capture with CaO in a 1.7 MWt pilot facility. *Energy Procedia* 37, 1–8. <https://doi.org/10.1016/j.egypro.2013.05.078>.
- Shirazi, A., Aminyavari, M., Najafi, B., Rinaldi, F., Razaghi, M., 2012. Thermal-economic-environmental analysis and multi-objective optimization of an internal-reforming solid oxide fuel cell-gas turbine hybrid system. *Int. J. Hydrog. Energy* 37, 19111–19124. <https://doi.org/10.1016/j.ijhydene.2012.09.143>.
- Singh, B., Strømman, A.H., Hertwich, E.G., 2011. Comparative life cycle environmental assessment of CCS technologies. *Int. J. Greenh. Gas Control* 5, 911–921. <https://doi.org/10.1016/j.ijggc.2011.03.012>.
- Steinbach, J., Staniaszek, D., 2015. Discount Rates in Energy System Analysis Discussion Paper. Buildings Performance Institute Europe (BPIE).
- Ströhle, J., Junk, M., Kremer, J., Galloy, A., Epple, B., 2014. Carbonate looping experiments in a 1 MW<sub>th</sub> pilot plant and model validation. *Fuel* 127, 13–22. <https://doi.org/10.1016/j.fuel.2013.12.043>.
- Tollefson, J., 2015. The 2°C dream. *Nature* 527, 436–438.

- Versteeg, P., Rubin, E.S., 2011. A technical and economic assessment of ammonia-based post-combustion CO<sub>2</sub> capture at coal-fired power plants. *Int. J. Greenh. Gas Control* 5, 1596–1605. <https://doi.org/10.1016/j.ijggc.2011.09.006>.
- Wang, X., Dai, Y., 2016. Exergoeconomic analysis of utilizing the transcritical CO<sub>2</sub> cycle and the ORC for a recompression supercritical CO<sub>2</sub> cycle waste heat recovery: a comparative study. *Appl. Energy* 170, 193–207. <https://doi.org/10.1016/j.apenergy.2016.02.112>.
- Yang, Y., Zhai, R., Duan, L., Kavosh, M., Patchigolla, K., Oakey, J., 2010. International journal of greenhouse gas control integration and evaluation of a power plant with a CaO-based CO<sub>2</sub> capture system. *Int. J. Greenh. Gas Control* 4, 603–612. <https://doi.org/10.1016/j.ijggc.2010.01.004>.
- ZEP, 2011. The Costs of CO<sub>2</sub> Capture, Transport and Storage. European Technology Platform for Zero Emission Fossil Fuel Power Plants.
- Zhang, Y., Li, H., Han, W., Bai, W., Yang, Y., Yao, M., Wang, Y., 2018. Improved design of supercritical CO<sub>2</sub> Brayton cycle for coal-fired power plant. *Energy* 155, 1–14. <https://doi.org/10.1016/j.energy.2018.05.003>.
- Zhao, M., Minett, A.L., Harris, A.T., 2013. Environmental Science of conventional pulverised-coal power plants for. *Energy Environ. Sci.* 6, 25–40. <https://doi.org/10.1039/c2ee22890d>.

## Nomenclature

$A_{HE}$ : heat exchanger surface area  
 $C_C$ : cost of CO<sub>2</sub> compressor  
 $C_{CCT}$ : investment cost of CCT  
 $C_{CT}$ : cost of cooling tower  
 $C_{Cal}$ : cost of calciner  
 $C_{CaLC}$ : investment cost of CaLC  
 $C_{CaLC,ex}$ : CaLC unit exploitation cost  
 $C_{Car}$ : cost of carbonator  
 $C_E$ : cost of CO<sub>2</sub> expander  
 $C_{EG}$ : cost of electric generator  
 $CF$ : capacity factor  
 $C_{FP}$ : cost of fuel preparation system  
 $C_{Fan}$ : cost of fan  
 $CF_t$ : annual cash flow  
 $C_{HE}$ : cost of heat exchanger  
 $C_{Inv}$ : investment cost  
 $C_{L\&O}$ : land and owner's cost  
 $C_{Op}$ : operating cost  
 $C_P$ : cost of CO<sub>2</sub> pump  
 $C_{SC,ex}$ : steam cycle exploitation cost  
 $C_{Tax}$ : income tax  
 $c_{chem}$ : unit price of chemical  
 $c_{CaCO_3}$ : unit price of fresh sorbent  
 $c_{Cal}$ : unit price of calciner  
 $c_{Car}$ : unit price of carbonator  
 $c_D$ : unit cost of disposal  
 $c_{FP}$ : unit price of the fuel preparation system  
 $c_{H_2O}$ : unit price of the water  
 $D$ : depreciation  
 $FCF$ : fixed charge factor  
 $FOM$ : fixed operating and maintenance cost  
 $HHV$ : higher heating value

$I_{El}$ : income from electricity sales  
 $I_{Sq}$ : salvage value  
 $I_{E\&PC}$ : engineering and project cost indicator  
 $I_{LC}$ : labour cost indicator  
 $i_{P\&C}$ : integration costs indicator  
 $i_{TASC}$ : total as-spent cost (TASC) multiplier  
 $LCOE$ : levelised cost of electricity  
 $\dot{m}_{AE}$ : equivalent mass flow rate of air  
 $\dot{m}_{Chem}$ : chemical flow rate for water treatment  
 $\dot{m}_{CaCO_3}$ : fresh sorbent make-up flow rate  
 $\dot{m}_{D,Ash}$ : disposed ash flow rate  
 $\dot{m}_{D,Sorb}$ : disposed sorbent flow rate  
 $\dot{m}_F$ : fuel flow rate  
 $NPV$ : net present value  
 $\dot{n}_{LR}$ : molar flow rate of solid looping  
 $\dot{n}_{MU}$ : molar flow rate of fresh limestone make-up  
 $P_{AUX}$ : total auxiliary power requirement  
 $P_{CCT}$ : auxiliary power of CCT  
 $P_{CaLC}$ : auxiliary power of CaLC  
 $P_{Fan}$ : fan break power  
 $P_G$ : gross power output  
 $P_N$ : net power output  
 $P_P$ : pump brake power  
 $p_{HE}$ : heat exchanger operating pressure  
 $Q_{Cal}$ : calciner heat flux  
 $Q_{Car}$ : carbonator heat flux  
 $RMU$ : relative sorbent make-up ratio  
 $r$ : discount rate  
 $r_{Tax}$ : income tax rate  
 $SFC$ : specific fuel cost  
 $TCR$ : total capital requirement  
 $\dot{V}_{H_2O}$ : flow rate of make-up water  
 $VOM$ : specific variable operating and maintenance cost  
 $\eta_N$ : net efficiency of power plant  
 $\eta_i$ : isentropic efficiency  
 $\tau$ : annual operating time

## Abbreviations

CaL: calcium looping  
 CaLC: calcium looping combustion  
 CCS: carbon capture and storage  
 CCT: CO<sub>2</sub> compression train  
 CGC: clean gas cooler  
 CO<sub>2</sub>-C: CO<sub>2</sub> compressor  
 CO<sub>2</sub>-E: CO<sub>2</sub> expander  
 CON: steam condenser  
 HHV: higher heating value  
 HTR: high-temperature recuperator  
 LCOE: levelised cost of electricity  
 LTR: low-temperature recuperator  
 NPV: net present value  
 SC: steam cycle  
 s-CO<sub>2</sub>: supercritical CO<sub>2</sub> cycle



2019-02-11

# Techno-economic feasibility assessment of calcium looping combustion using commercial technology appraisal tools

Michalski, Sebastian

Elsevier

---

Sebastian Michalski, Dawid P. Hanak and Vasilije Manovic Techno-economic feasibility assessment of calcium looping combustion using commercial technology appraisal tools.

Journal of Cleaner Production, Volume 219, 10 May 2019, Pages 540-551

<https://doi.org/10.1016/j.jclepro.2019.02.049>

*Downloaded from Cranfield Library Services E-Repository*